STUDY OF EUTECTIC FORMATION

August 1984

Final Report on Contract NAS8-34887
Reporting Period: 3 May 1982 to 2 August 1984

Prepared for
George C. Marshall Space Flight Center
National Aeronautics and Space Administration

Prepared by
William R. Wilcox, G.F. Eisa, V. Baskaran and Donald C. Richardson
Department of Chemical Engineering
Clarkson University
Potsdam, New York 13676

Sponsored by
Microgravity Science and Applications Division
National Aeronautics and Space Administration
Washington, DC 20546

CONTENTS

ABSTRACT

The object of this contract was to help understand why MnBi-Bi eutectic solidified in space has a finer microstructure than when it is solidified on earth under otherwise identical conditions.

A theory was developed for the influence of convection on the microstructure of lamellar eutectics. Convection is predicted to produce a coarser microstructure, especially at low freezing rates and large volume fractions of the minority phase. Similarly convection is predicted to lower the interfacial undercooling, especially at low freezing rates.

Experiments using spin-up/spin-down (accelerated crucible rotating technique) were performed on the Mn-Bi eutectic. This stirring had a dramatic effect on the microstructure, not only making it coarser but at low freezing rates also changing the morphology of the MnBi. The coarsering persisted to moderately high freezing rates. At the lowest freezing rate, vigorous stirring caused the MnBi to be concentrated at the periphery of the ingot and absent along the center.

Progress was made on developing a technique for revealing the three-dimensional microstructure of the MnBi eutectic by time-lapse videotaping while etching.

INTRODUCTION

The MnBi-Bi eutectic forms fibers of MnBi in a matrix of bismuth when it is directionally solidified. Larson and Pirich at Grumman Aerospace Corporation showed that solidification in space at 30 and 50 cm/hr causes the average fiber spacing λ to be about half the value for solidification on earth, under otherwise identical conditions (1). We have been collaborating with Larson and Pirich to try to find an explanation for this surprising phenomenon. It appears that neither an altered temperature gradient (2) nor a fluctuating freezing rate (3) are responsible for changing λ. In the present work we have concentrated on investigating the direct influence of convection on λ. Both theory and experiments have been performed. A masters thesis and two papers have already resulted from this research. It should be completed near the end of 1984 to yield a doctoral thesis and two additional papers.

We have also been developing a technique for slowly etching through the MnBi-Bi eutectic while time-lapse videotaping. Played back at normal speed, such videotapes should give a good picture of MnBi fiber branching, termination, nucleation, and meandering. This should provide additional insight into the mechanism behind the change in λ with gravity.

THEORY
(V. Baskaran and G.F. Eisa)

The two attached papers summarize the results of Mr. Baskaran in his 1983 M.S. thesis. He used numerical techniques on the computer to solve for the concentration field in front of a growing lamellar eutectic of composition W_e and lamellar spacing λ. The approach of Hunt and Jackson (4) was used to convert the computed concentration field to

$$\lambda/\lambda_o = 1 + 0.00034\Gamma_o^2 \qquad (1)$$

for a 50 volume % eutectic (W_e = 0.50). Here λ is the lamellar spacing with convection, λ_o the value without convection, $\Gamma_o = G_u\lambda_o^2/D$, G_u is the transverse convection velocity gradient at the interface and D is the diffusion coefficient in the melt.

In the Jackson-Hunt approach used to develop Eq. (1), it is assumed that λ takes on the value giving the smallest total undercooling ΔT at the solid-liquid interface. The undercooling ΔT is the sum of two parts, one for surface tension which is inversely proportional to λ, and one proportional to the deviation of the interfacial composition from the eutectic. This latter part is decreased by convection, thereby causing λ to increase. (This is in the same direction as the Grumman experimental observation on MnBi).

Substitution of reasonable values for G_u and D into Eq. (1) revealed that the buoyancy-driven natural convection expected in the vertical Bridgman-Stockbarger technique is insufficient to explain the two-fold change in λ observed by solidifying MnBi in space. It was speculated that the effect might be much larger for small W_e, much larger for fibrous eutectics (the theory is for lamellar eutectics), or much larger if the MnBi fibers extend out into the melt beyond the Bi.

To investigate the influence of small W_e, Mr. Eisa has used Mr. Baskaran's program for W_e = 0.1 and 0.3. Figures 1 to 6 show typical isoconcentration plots for $\Lambda = \lambda V/D = 0.05$ and $\Gamma = G_u\lambda^2/D = 0$ or 500, where V is the growth velocity. Figures 7 to 9 compare interfacial concentrations ($W_{z=0}$) from our convection-free numerical results with the analytical results of Hunt and Jackson. Figures 10 to 12 show average interfacial compositions $\overline{W}_i$ in the absence of convection vs. Λ. From the foregoing we see that the numerical results are very good for small Λ. Consequently Λ = 0.05 was used to compute λ/λ_o.

We found that the methods used in the attached paper by Baskaran and Wilcox are correct only for $W_e = 0.5$, a 50 volume % eutectic. For other values of W_e it turns out that the influence of convection on the average interfacial composition is different for phase α and phase β. Thus the treatment on p.5 and p.6 of Baskaran-Wilcox needs to be altered as follows:

Define $$\Delta_\alpha = (\bar{W}_{i\alpha}-W_e)_0 - (\bar{W}_{i\alpha}-W_e) \quad (2)$$

$$\Delta_\beta = (\bar{W}_{i\beta}-W_e)_0 - (\bar{W}_{i\beta}-W_e) \quad (3)$$

From the analytical solution of Jackson-Hunt (4),

$$(W_{i\alpha}-W_e)_0 = A_\alpha \Lambda \quad (4)$$

$$(W_{i\beta}-W_e)_0 = A_\beta \Lambda \quad (5)$$

where $$A_\alpha = P/(1-W_e) \quad (6)$$

$$A_\beta = P/W_e \quad (7)$$

$$P = \sum_{n=1}^{\infty} (1/n\pi)^3 \sin^2(n\pi(1-W_e)) \quad (8)$$

The undercooling ΔT over each phase is the sum of compositional undercooling and curvature undercooling:

$$\Delta T_\alpha = m_\alpha(\bar{W}_{i\alpha}-W_e) + C_{2\alpha}/S_\alpha$$

$$= m_\alpha A_\alpha \Lambda - m_\alpha \Delta_\alpha + C_{2\alpha}/S_\alpha \quad (9)$$

$$\Delta T_\beta = m_\beta A_\beta \Lambda - m_\beta \Delta_\beta + C_{2\beta}/S_\beta \quad (10)$$

where m_α and m_β are slopes of the liquidi lines for α and β phases at the eutectic, and $C_{2\alpha}$ and $C_{2\beta}$ are constants relating lamellar widths $2S_\alpha$ and $2S_\beta$ to the melting point depressions due to curvature.

Following Jackson-Hunt we add $\Delta T_\alpha/m_\alpha$ and $\Delta T_\beta/m_\beta$ and assume $\Delta T_\alpha = \Delta T_\beta = \Delta T$ to obtain Equation 17 on p.6 of the attached paper by Baskaran and Wilcox;

$$\Delta T = C_1 A\Lambda - C_1\Delta + C_2/\lambda \tag{11}$$

Now however the constants in this equation are given by:

$$C_1 = 1/(1/m_\alpha + 1/m_\beta) \tag{12}$$

$$A = P/W_e(1-W_e) \tag{13}$$

$$\Delta = \Delta_\alpha + \Delta_\beta \tag{14}$$

$$C_2 = 2(m_\beta C_{2\alpha}/(1-W_e) + m_\alpha C_{2\beta}/W_e)/(m_\beta + m_\alpha) \tag{15}$$

The subsequent equations and calculation methods in Baskaran-Wilcox are unchanged, only using these new definitions above.

Figures 13 and 14 show Δ_α and Δ_β vs. Γ for all three values of W_e. Figure 15 shows Δ vs. Γ. Figure 16 gives λ/λ_o vs. Γ_o. Notice that convection is predicted to have a smaller effect on λ for small W_e than for large W_e.

In the Baskaran-Wilcox paper, values of G_u, and thereby Γ_o and λ/λ_o, are estimated for typical crystal growth situations. While λ/λ_o can be large under some conditions, it is not predicted to be large for vertical Bridgman-Stockbarger growth in a small diameter ampoule, as done by Larson and Pirich.

Larson and Pirich claim to have observed a change in interfacial undercooling ΔT in going from solidification on earth to solidification in space. Our theoretical results can be used to predict this change as well. The minimum undercooling ΔT_{min} (vs. λ) is presumably what is observed. It can be found by substitution of Equation (21) of Baskaran-Wilcox into the present Equation (11), to yield:

$$\begin{aligned} 2(\Delta T)_{min}/(\Delta T)_{min,0} &= (1-f/A-(2\Gamma/A)(df/d\Gamma))^{1/2} \\ &\quad + (1-f/A)/(1-f/A-(2\Gamma/A)(df/d\Gamma))^{1/2} \\ &= g(\Gamma_o) \end{aligned} \tag{16}$$

where $f = \Delta/\Lambda$, g is defined as the RHS of Eq. (16), and $(\Delta T)_{min,0}$ is the minimum undercooling in the absence of convection ($\Gamma = 0$; via Jackson-Hunt). For $W_e = 0.5$ preliminary data yields a correlation of

$$g/2 = 1\text{-}0.0023\Gamma_o = 1\text{-}0.0023\ G_u\lambda_o^2/D$$

$$= (\Delta T)_{min}/(\Delta T)_{min,0} \qquad (17)$$

Noting that

$$\lambda_o^2 V = C_2 D/C_1 A \qquad (18)$$

and that

$$(\Delta T)_{min,0} = 2(C_2 C_1 AV/D)^{1/2} \qquad (19)$$

we find that

$$(\Delta T)_{min}/(\Delta T)_{min,0} = 1\text{-}0.0023\ C_2 G_u/C_1 A(VD)^{1/2} \qquad (20)$$

and

$$\Delta T_{min} = 2(C_2 C_1 A)^{1/2}((V/D)^{1/2} - 0.0023(C_2 G_u/C_1 A(VD)^{1/2}\ , \qquad (21)$$

Apparently Larson and Pirich have not yet compared this prediction with their experimental results.

SPIN-UP/SPIN-DOWN EXPERIMENTS
(G.F. Eisa)

Eutectic mixtures of Mn/Bi were directionally solidified in 9 mm ID glass ampoules using the apparatus of Ref. 2. During each run the ampoule was translated at a constant rate from the heater into the cooler. Every few cm a different stirring intensity was initiated, either no rotation, 100 RPM or 200 RPM about the ampoules axis. At 100 RPM the rotation was stopped for 4.5s and started for 4.5s. At 200 RPM 3s was used. Figures 17 to 30 show micrographs of cross sectional slices of these ingots. Stirring has a large effect on the microstructure at all freezing rates.

Quantitative analysis of the microstructure and comparison with theory has not yet been performed. However qualitatively we see two discrepancies with theory. First of all, at low freezing rates at 200 RPM stirring, we found no MnBi along the center of the ingot. There is no theoretical explanation for this.

Second, the influence of convection on microstructure persists to high freezing rates. Theory predicts that the effect of convection should die out quickly as freezing rate is increased.

ETCHING EXPERIMENTS
(D.C. Richardson)

The purpose of this research project was to reveal the three dimensional microstructure of the eutectic MnBi/Bi. Several methods to expose the MnBi rod structure for the Bi matrix were examined. Only electrochemical etching techniques were considered viable. Thus an exploration for a proper electrochemical macro etching solution was begun.

A special transparent electrochemical cell (Struers Visopol) was obtained to observe the microstructure using normal optics. After receipt of the Struers Visopol, it was found that longer working distance optics are required. A B-L microzoom microscope was obtained. The microscope was fitted with a time-lapse video system to record the process of electrochemical etching of the Mn/Bi/Bi.

The criteria for the development of a macro etching solution are:

* the etchant should produce good all-around results, should be applicable to the material under study and should reveal a great variety of structural characteristics and irregularities.
* the etchant should be simple in composition, inexpensive, and easy to prepare.

* the etchant should be stable during use and storage.

* the etchant must be safe to use and should not produce noxious odors.

In particular for MnBi/Bi eutectic three-dimensional microstructure studies the additional criteria must be added:

* the etchant must remain transparent for use with an optical microscope.

* the etchout should produce a relatively flat surface as material is removed.

Many etchants have been tried. A brief description of three of these etchants and their use with MnBi/Bi eutectic follows.

The most widely used etchant for Bi is a mixture of glycerol, glacial acetic acid and nitric acid. The formation of gaseous NO_x rendered it unsuitable for optical viewing.

Another popular Bi etchant is potassium iodine with hydrochloric acid Here there was formation of iodine gas which made it hard to get clear pictures. The surface of the samples were badly pitted as well.

The best etching solution to date has been a mixture of sulfuric and phosphoric acids with water. It is optically clear and the surface is etched uniformly.

REFERENCES

1. R.G. Pirich and D.J. Larson, p. 523 in "Materials Processing in the Reduced Gravity Environment of Space," edited by G.E. Rindone, Elsevier (1982).

2. P.S. Ravishankar, W.R. Wilcox and D. Larson, Acta Met. 28, 1583 (1980).

3. W.R. Wilcox, K. Doddi, M. Nair and D.J. Larson, Adv. Space Res. 3, 79 (1983).

4. K.A. Jackson and J.D. Hunt, Trans. AIME 236, 1129 (1966).

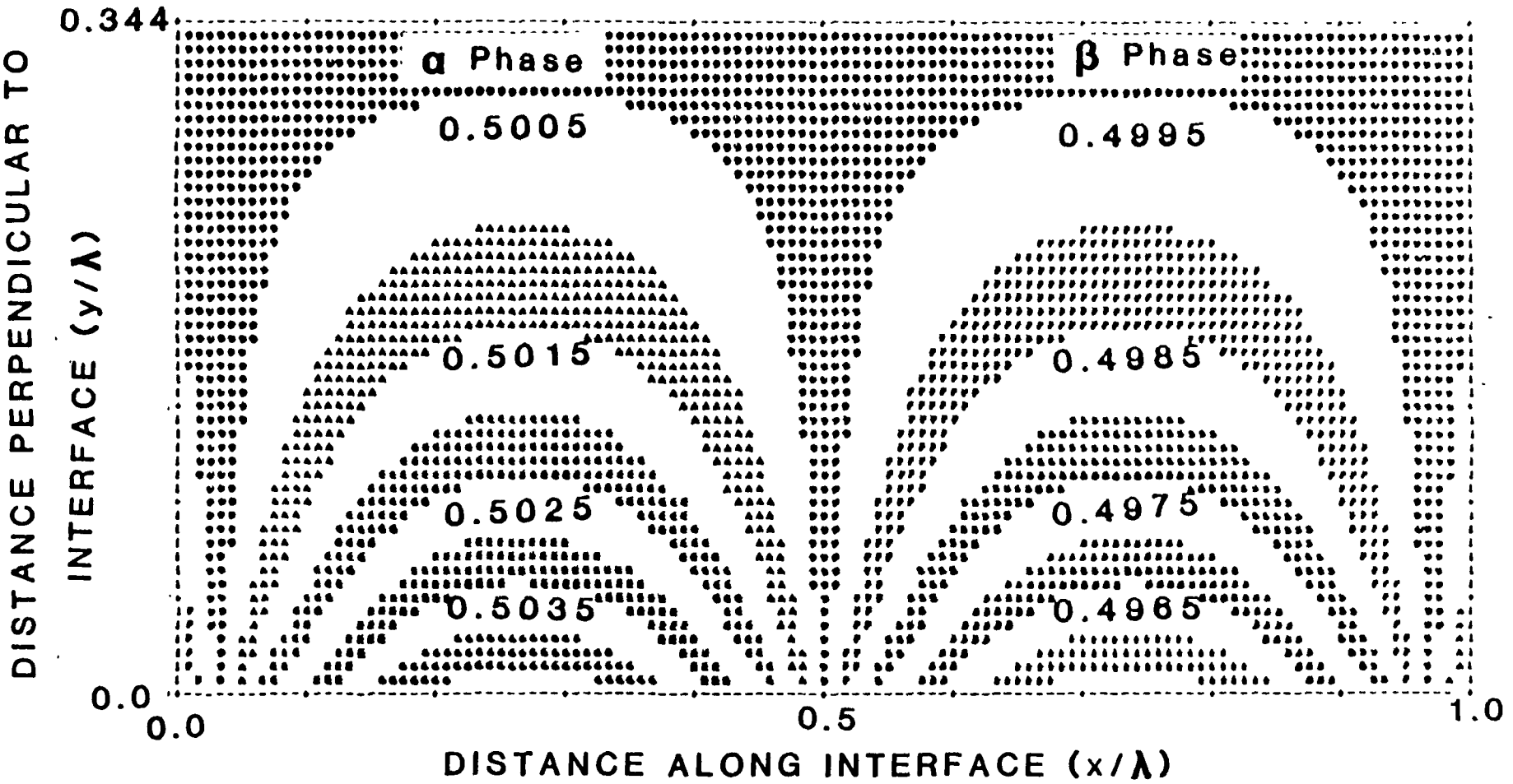

Figure 1. Isoconcentration lines from numerical solution for $W_e = 0.5$, $\Lambda = 0.05$ and $\Gamma = 0$ (no convection).

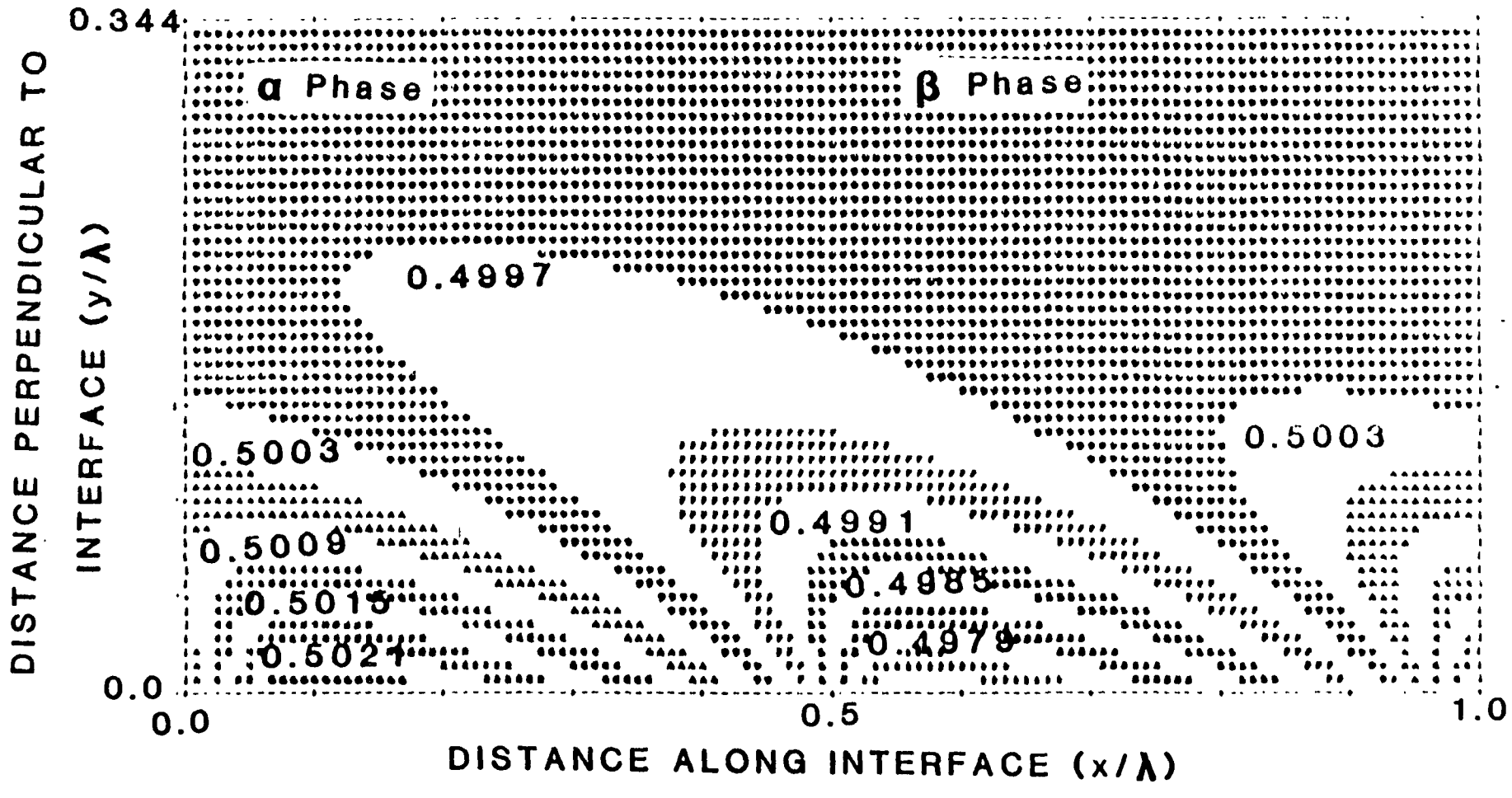

Figure 2. Results for W_e = 0.5, Λ = 0.05, Γ = 500. Transverse convective flow from right to left.

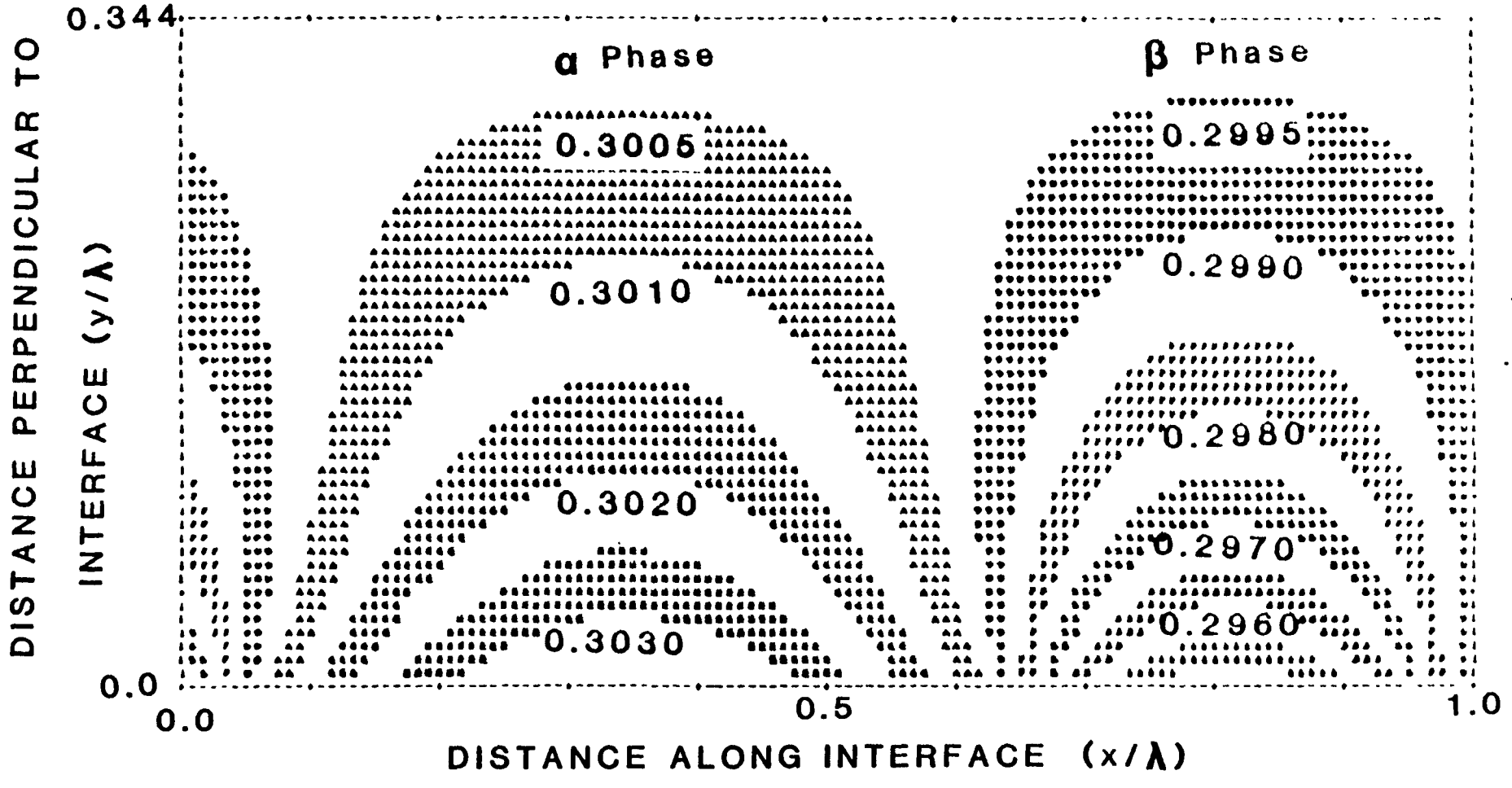

Figure 3. Results for $W_e = 0.3$, $\Lambda = 0.05$, $\Gamma = 0$.

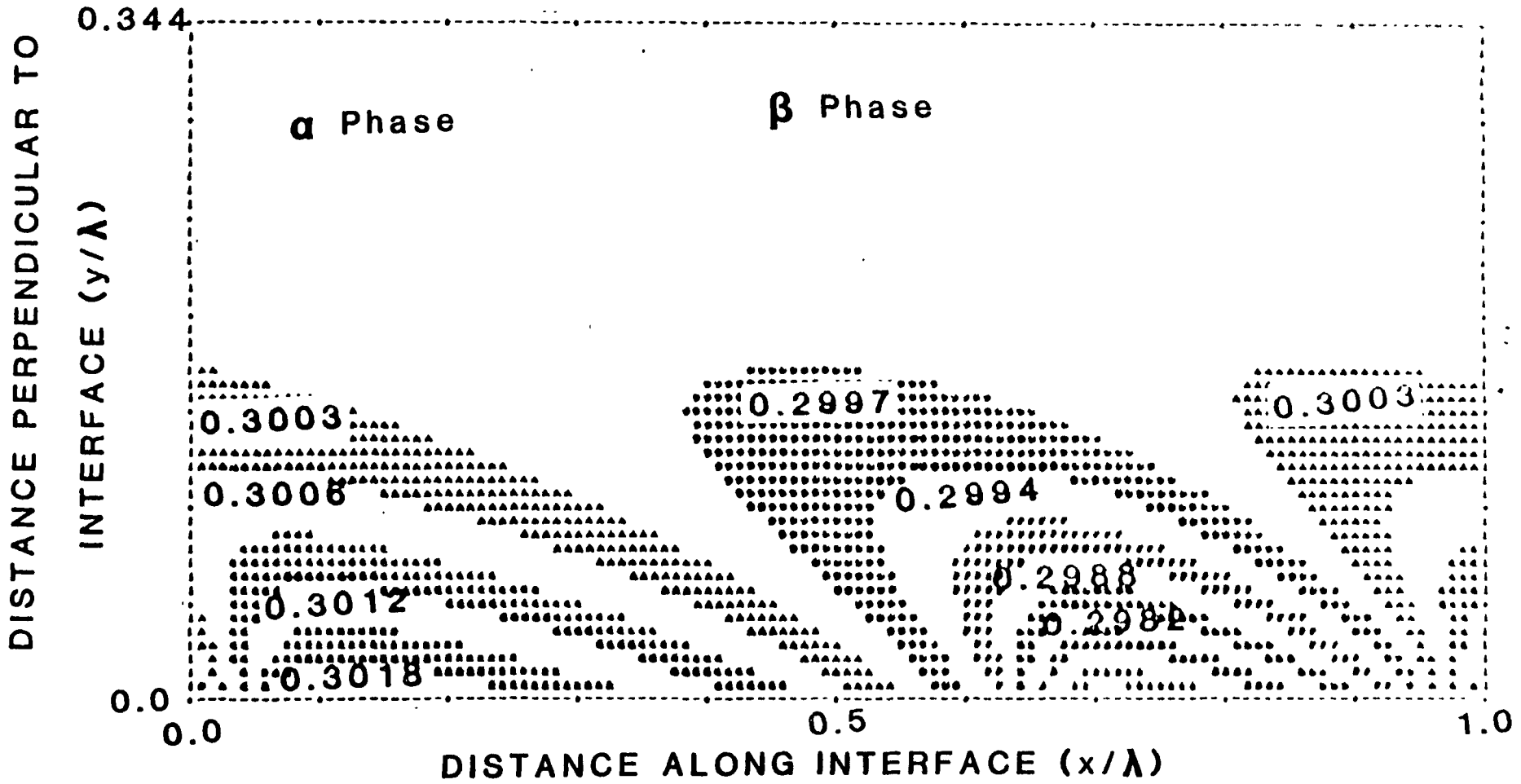

Figure 4. Results for W_e = 0.3, Λ = 0.05, Γ = 500.

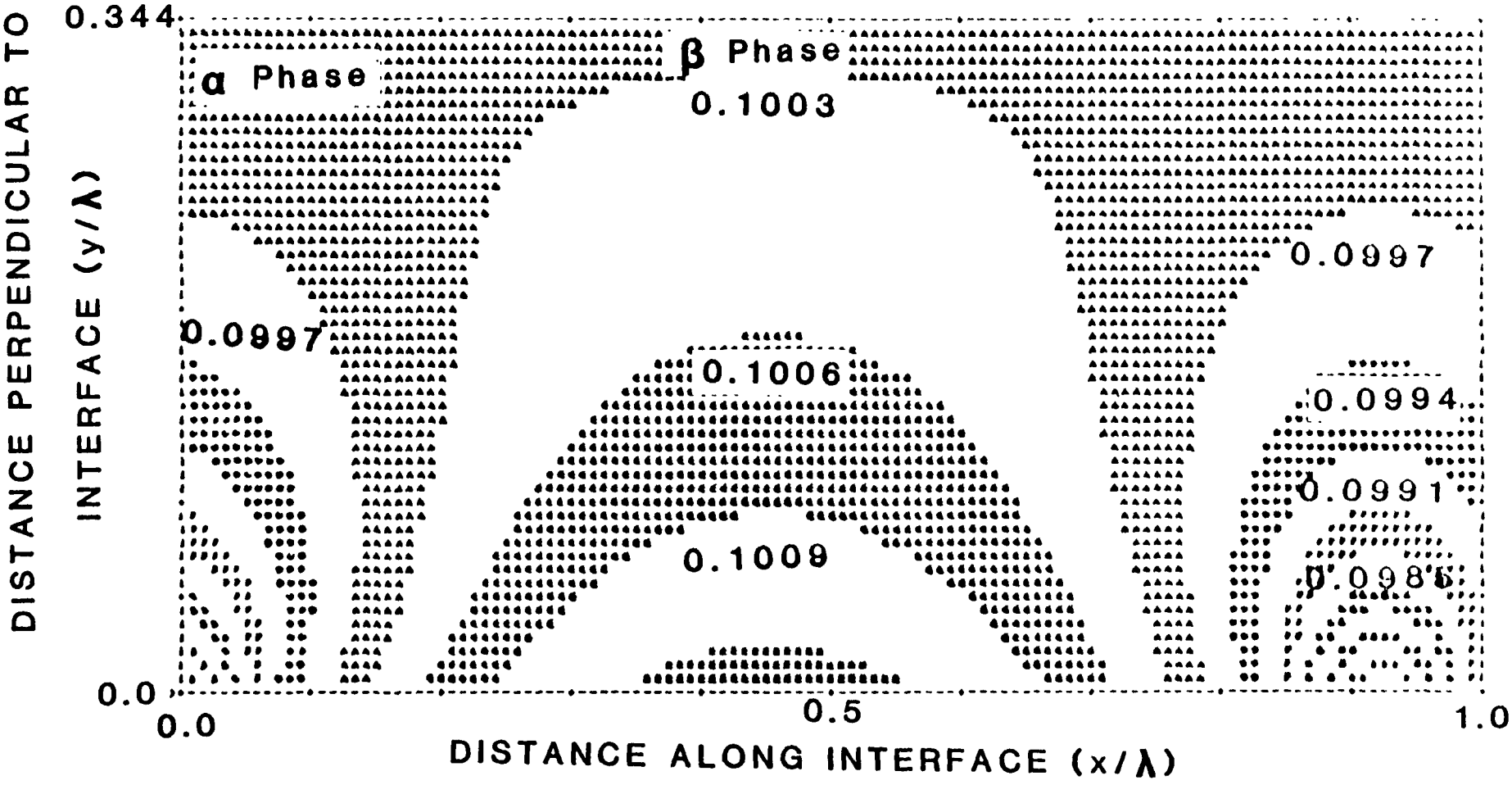

Figure 5. Results for $W_e = 0.1$, $\Lambda = 0.05$, $\Gamma = 0$.

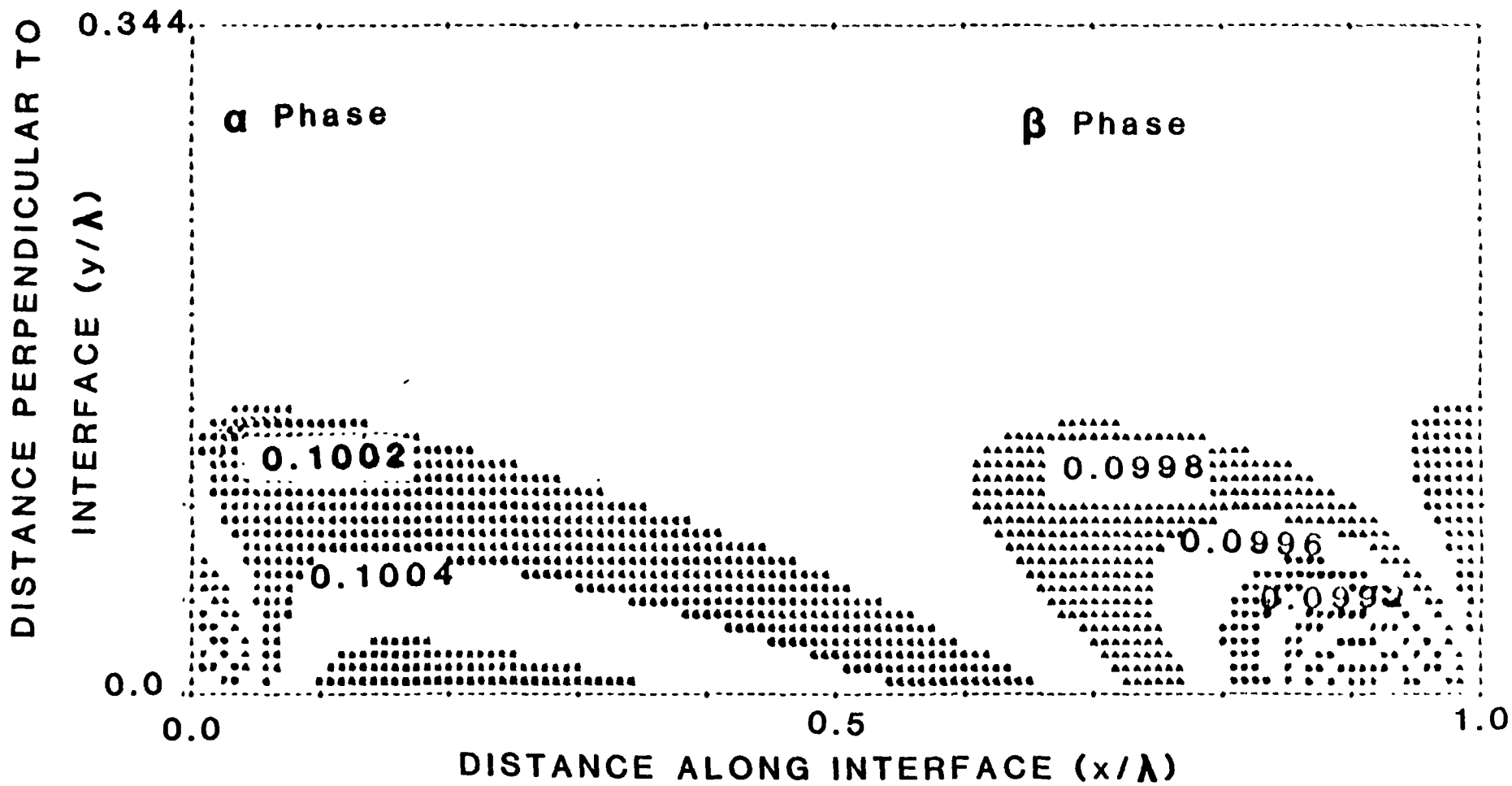

Figure 6. Results for W_e = 0.1, Λ = 0.05, Γ = 500.

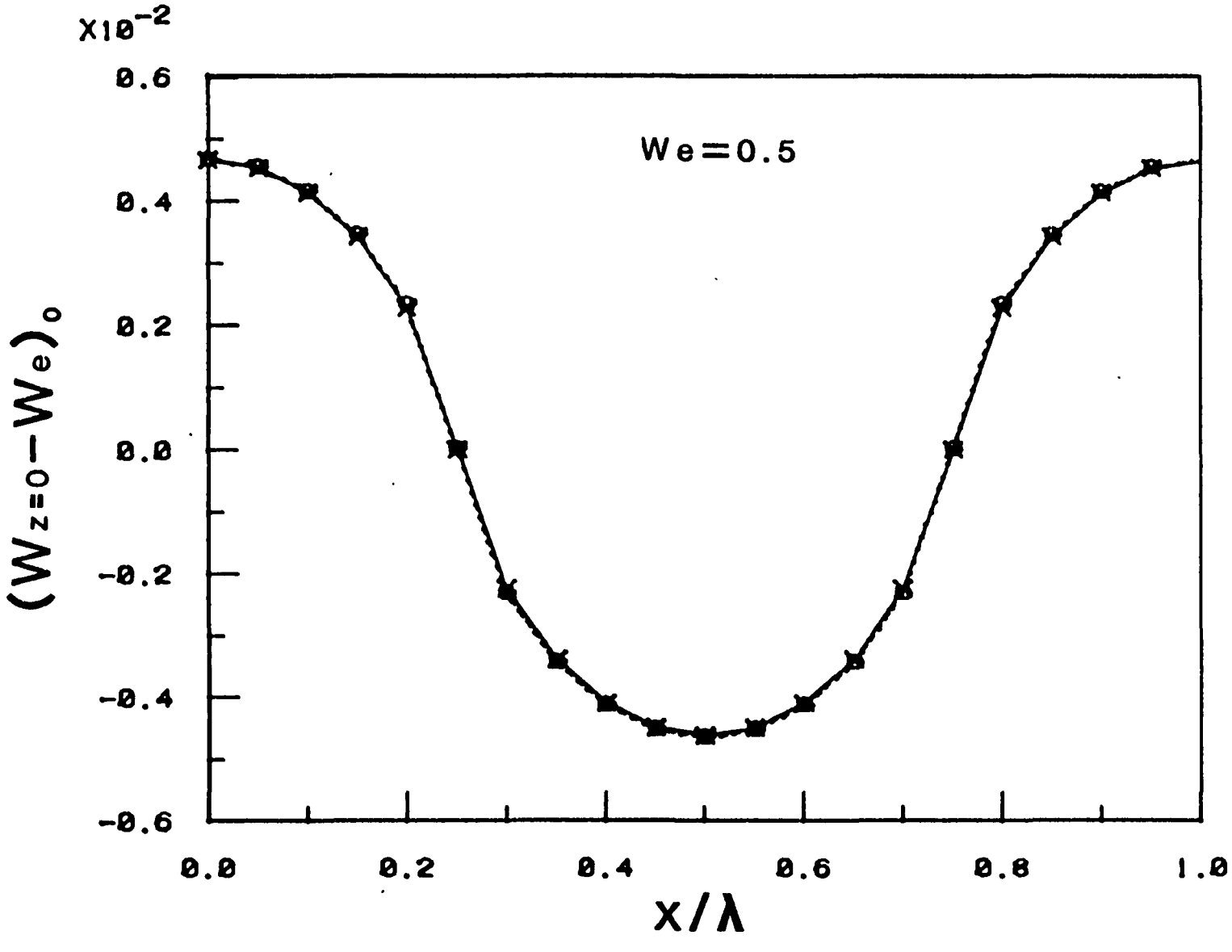

Figure 7. Deviation of interfacial melt concentration $W_{z=0}$ from eutectic, $W_e = 0.5$, vs. distance along interface X in the absence of convection for $\Lambda = 0.05$.

O - Present numerical results.

X - Jackson-Hunt analytical results.

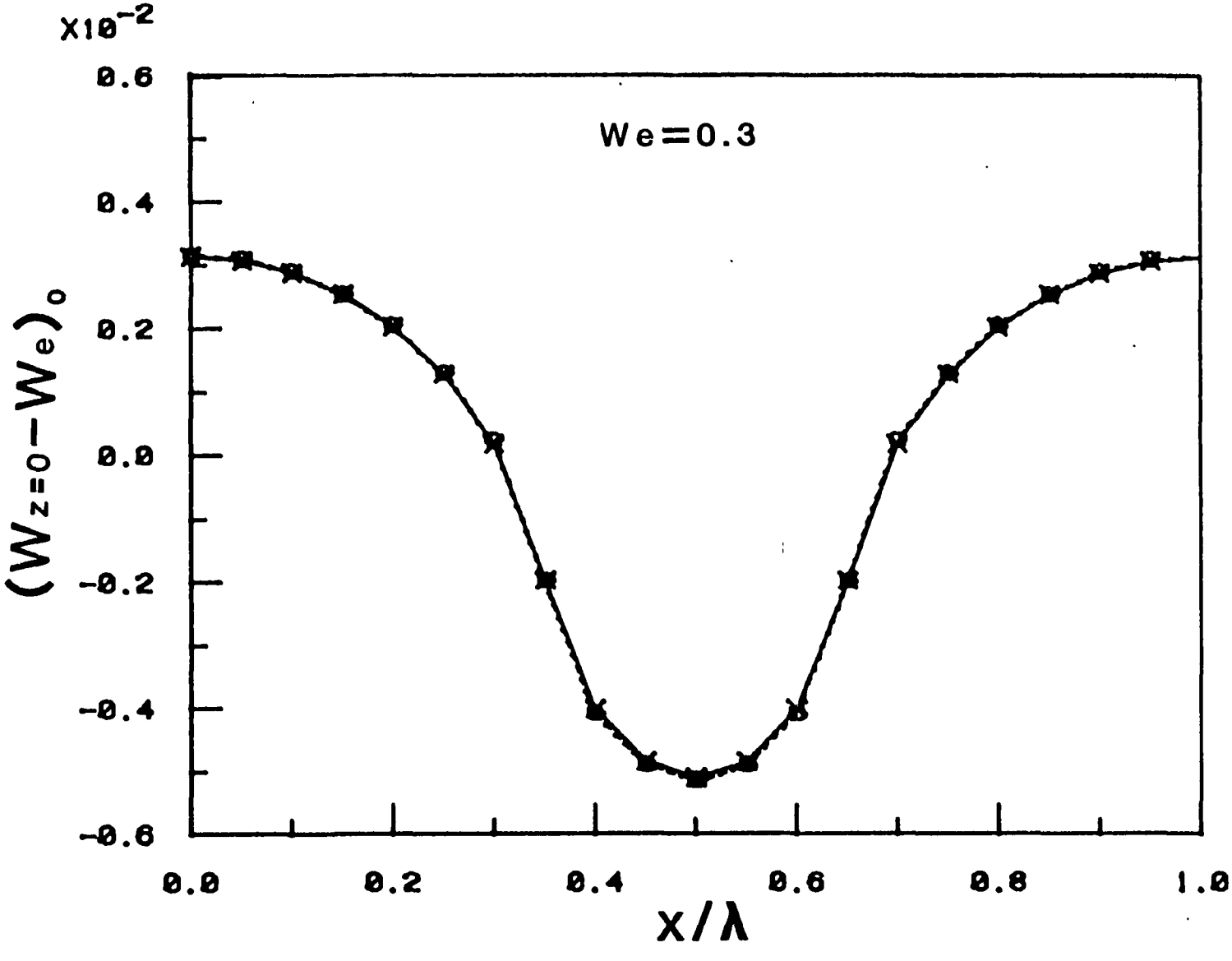

Figure 8. Comparison of interfacial melt concentrations from numerical results (O) with analytical results (X) for W_e = 0.3, Λ = 0.05, Γ = 0..

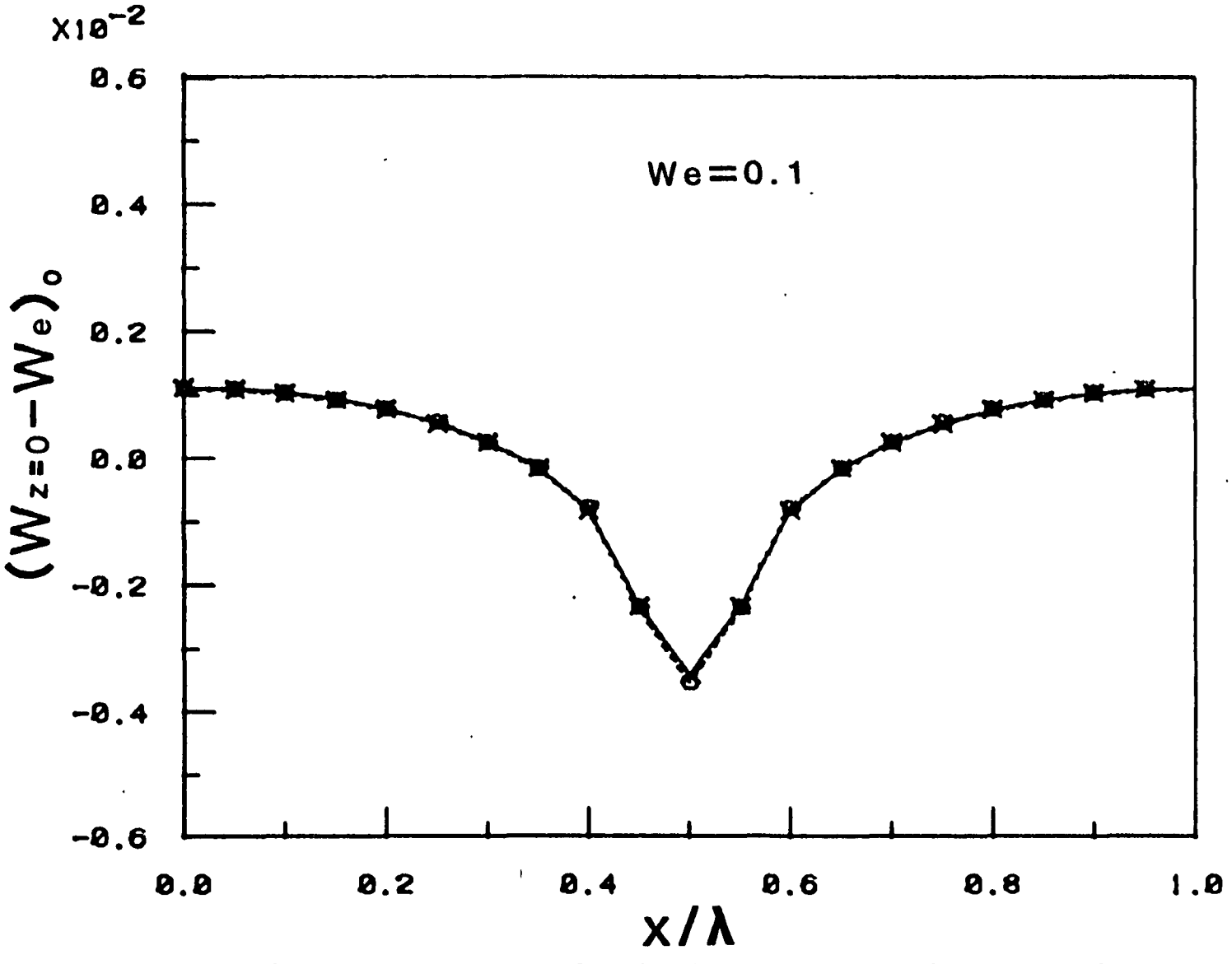

Figure 9. Comparison of interfacial melt concentrations from numerical results (0) with analytical results (X) for W_e = 0.1, Λ = 0.05, Γ = 0.

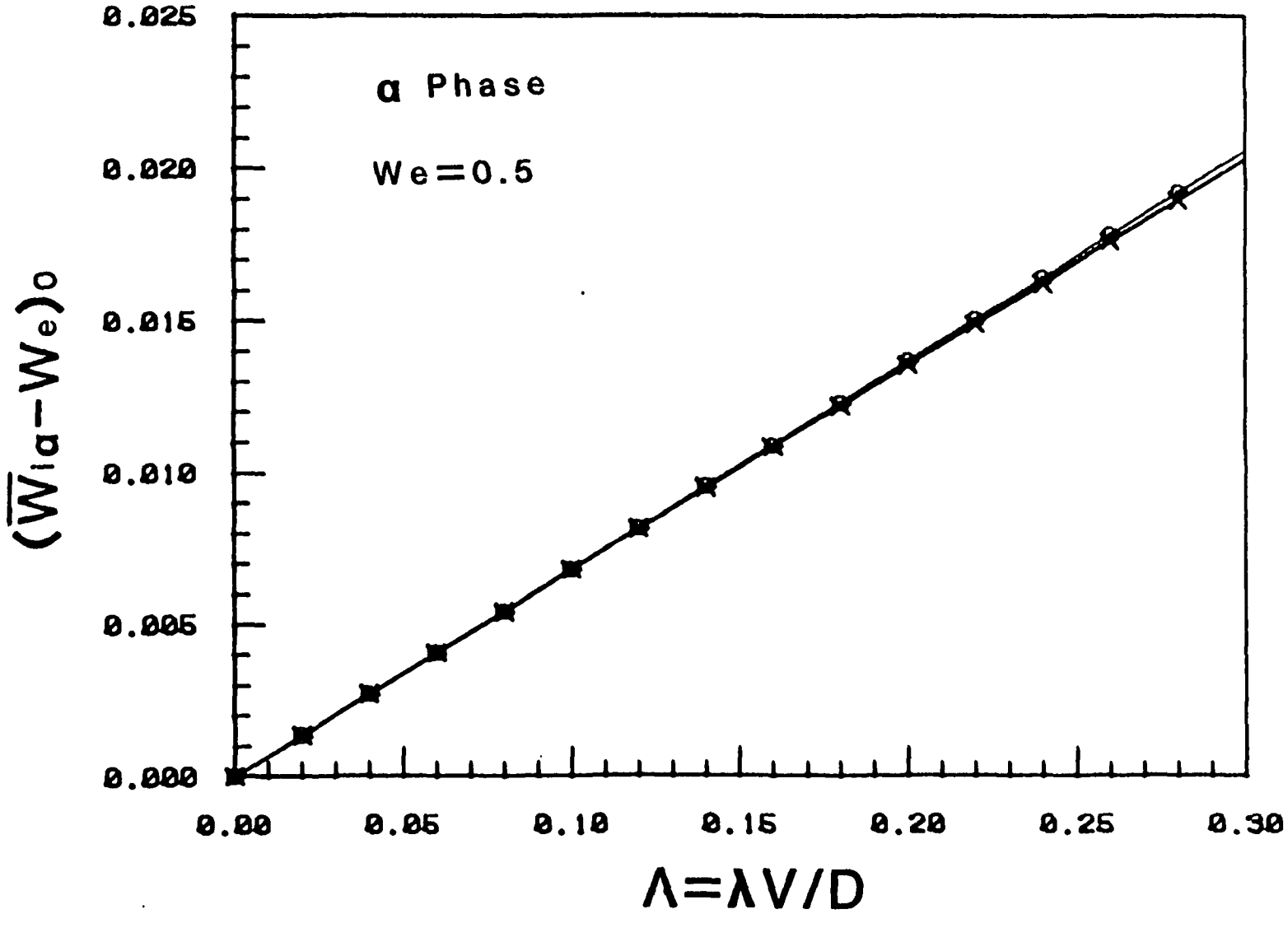

Figure 10. Average interfacial melt composition $\overline{W}_{i\alpha}$ over the α phase for $W_e = 0.5$ and $\Gamma = 0$.

O - Numerical

X - Analytical

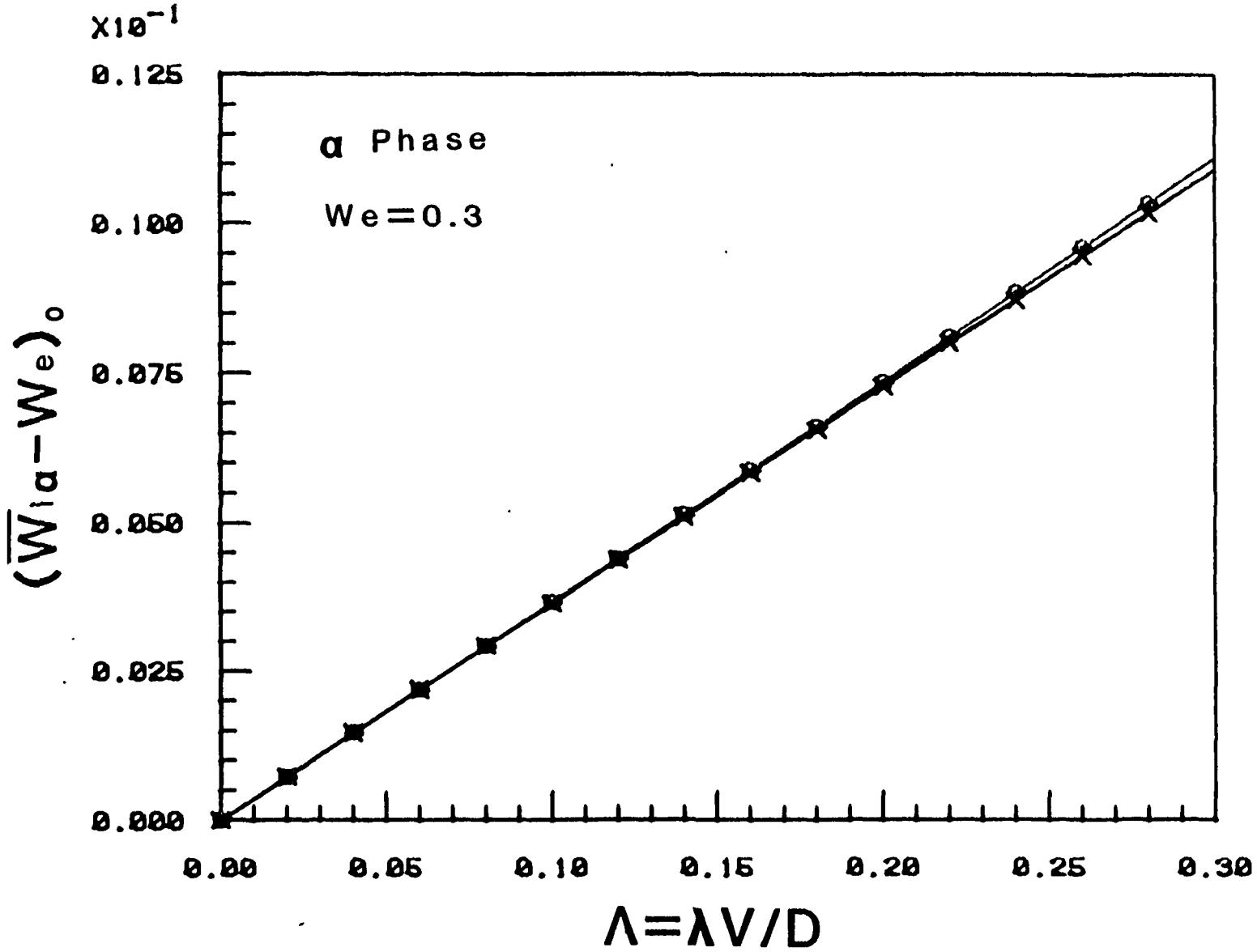

Figure 11. Average interfacial melt concentration over α phase for W_e = 0.3 and Γ = 0.

O - Numerical

X - Analytical

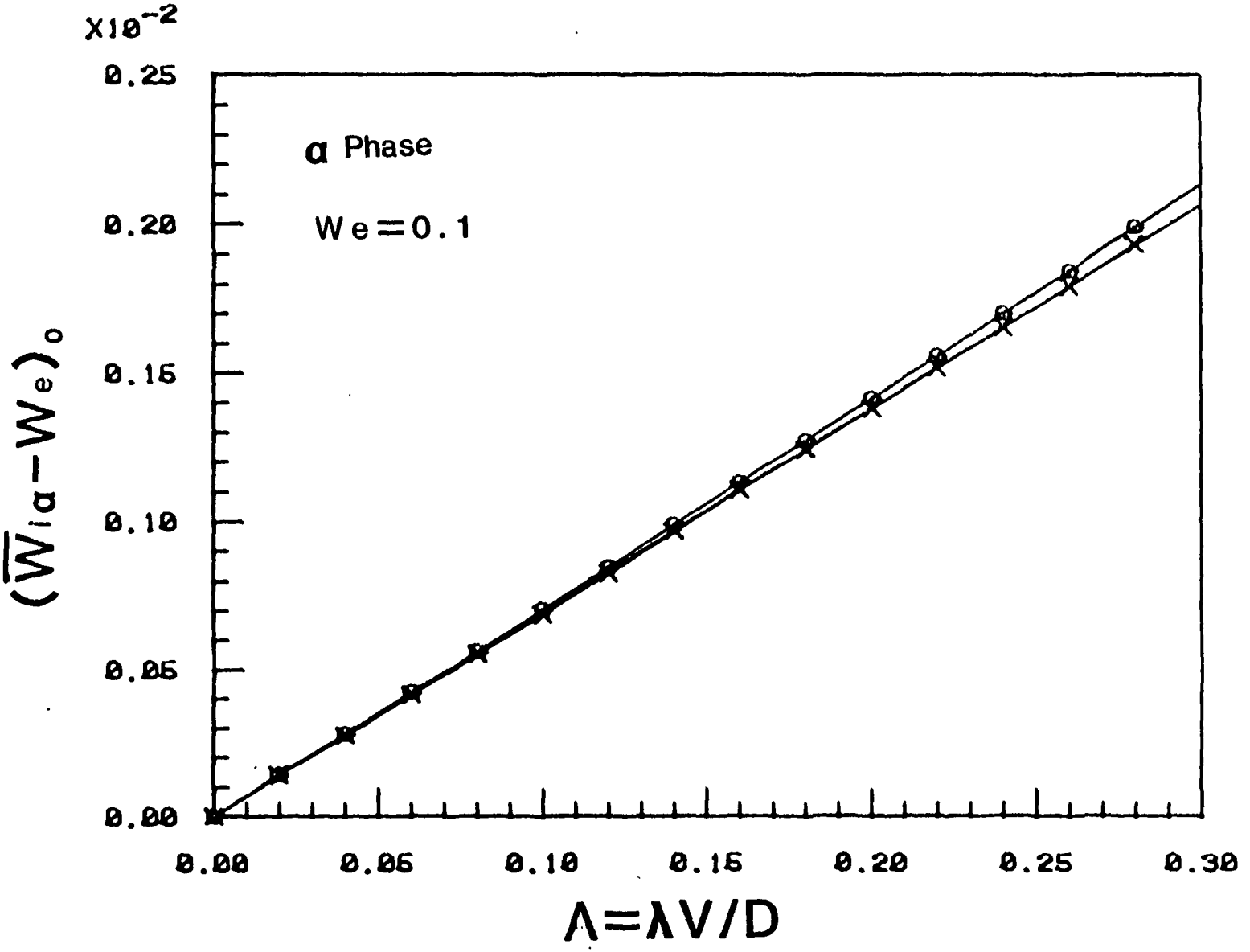

Figure 12. Average interfacial melt concentration over phase α for W_e = 0.1 and Γ = 0.

O - Numerical

X - Analytical

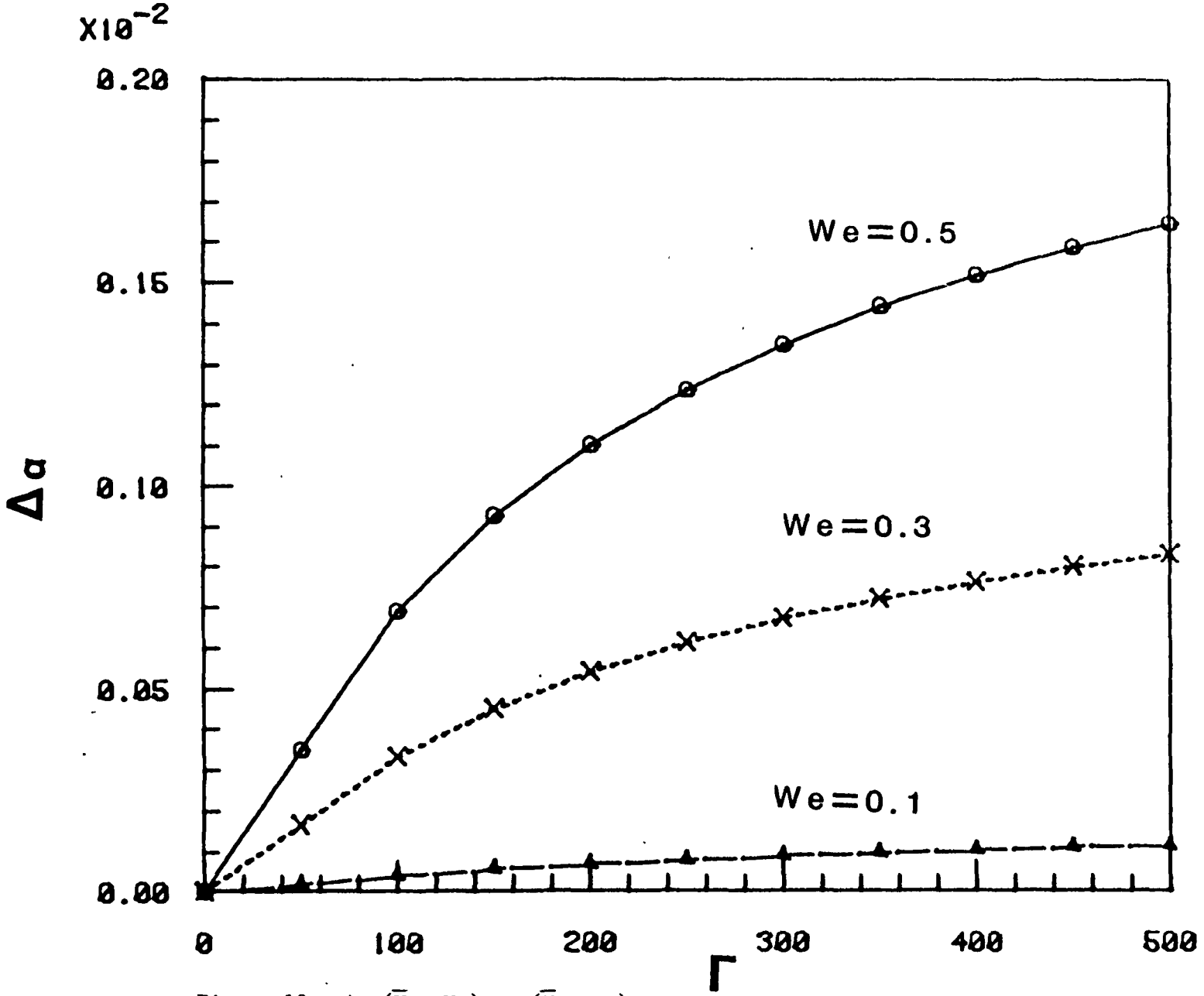

Figure 13. $\Delta_\alpha\ (\bar{W}_{i\alpha}-W_e)_0 - (\bar{W}_{i\alpha}-W_e)$ vs. Γ for $\Lambda = 0.05$.

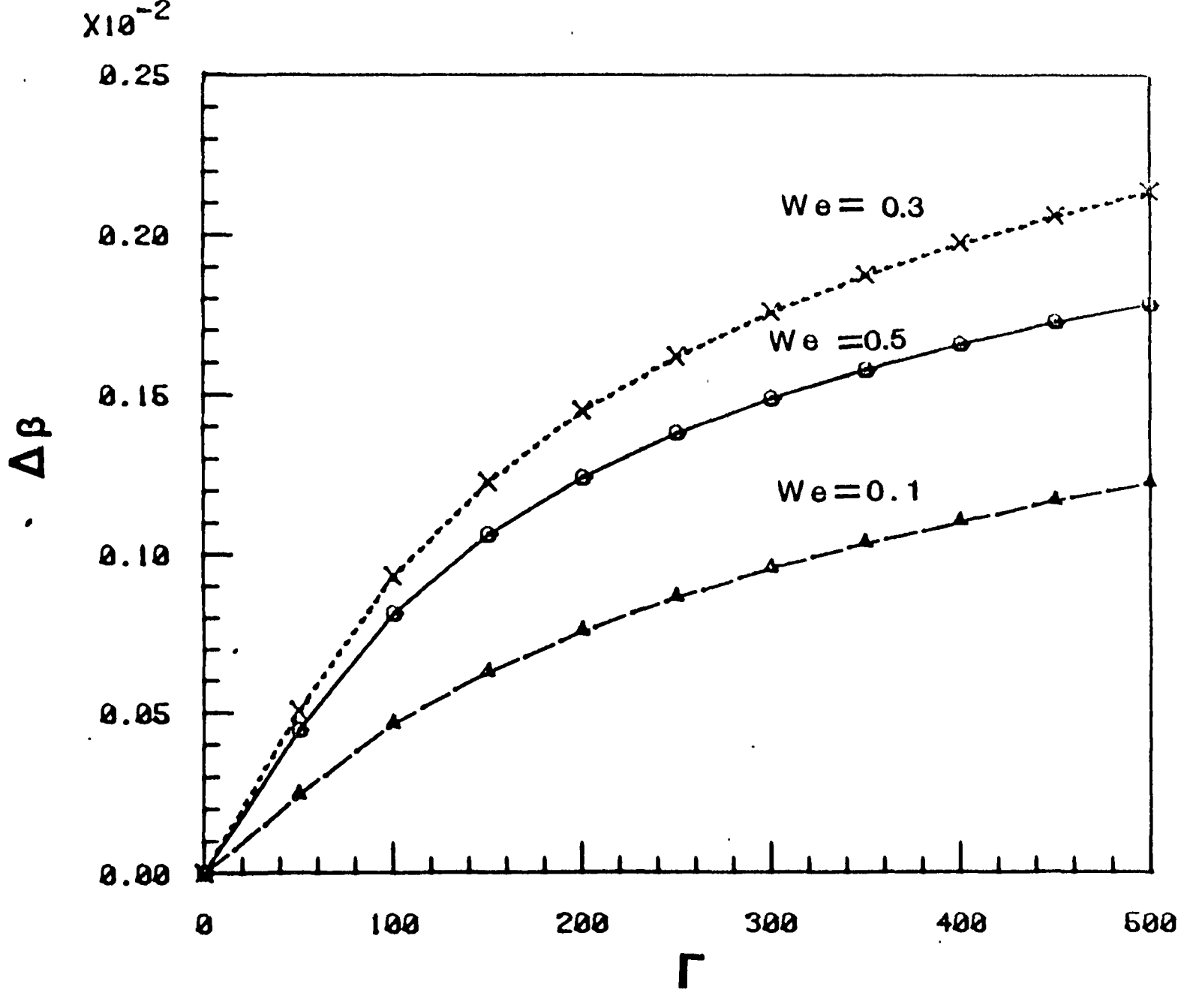

Figure 14. Δ_β vs. Γ for Λ = 0.05.

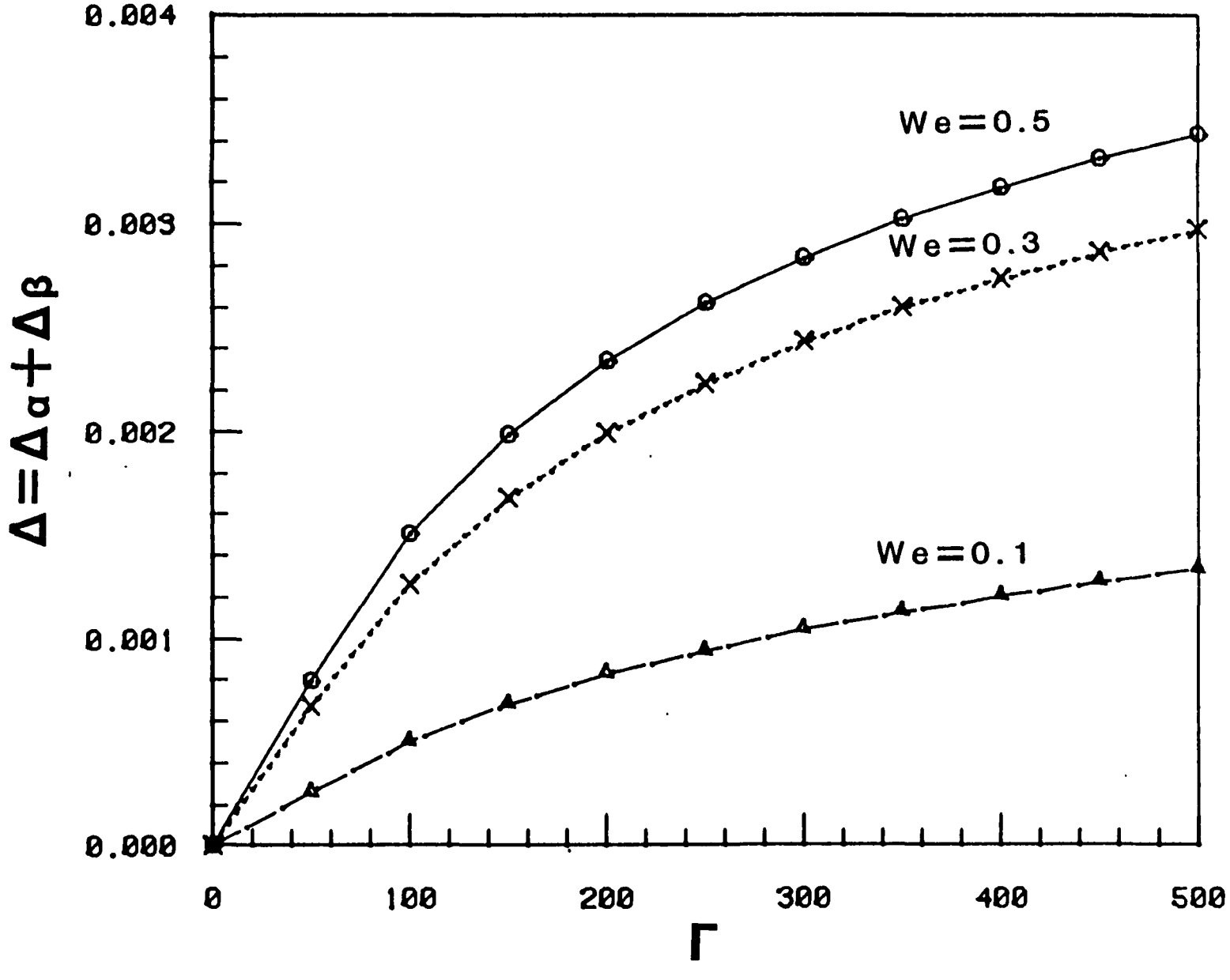

Figure 15. $\Delta = \Delta_\alpha + \Delta_\beta$ vs. Γ for $\Lambda = 0.05$.

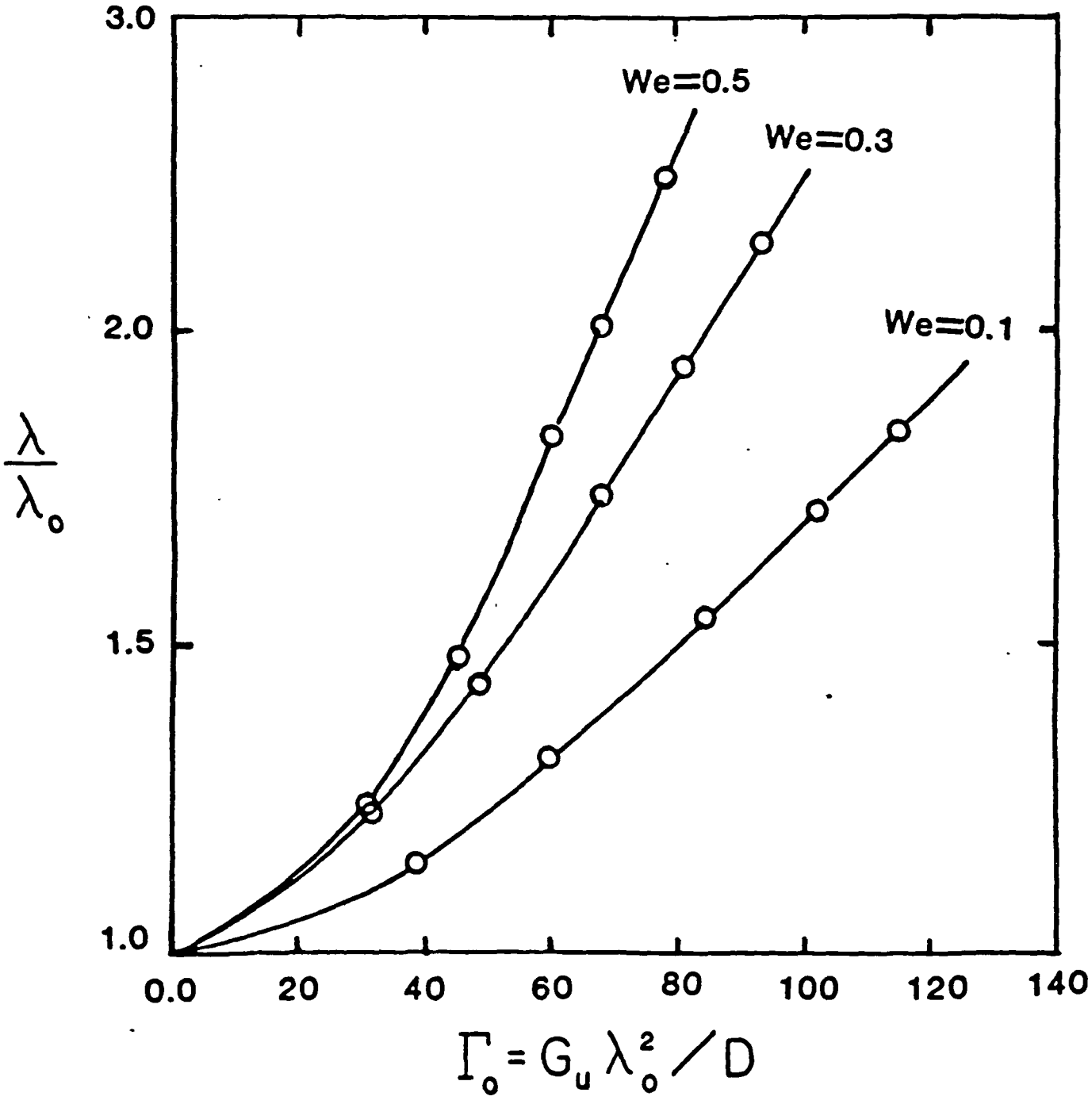

Figure 16. λ/λ_o vs. Γ_o.

(a)

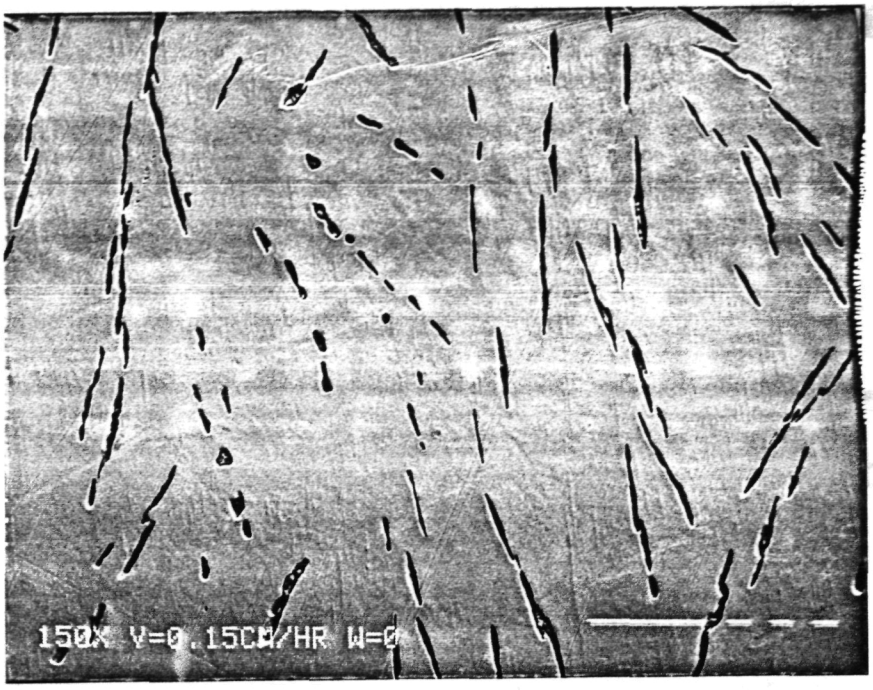

(b)

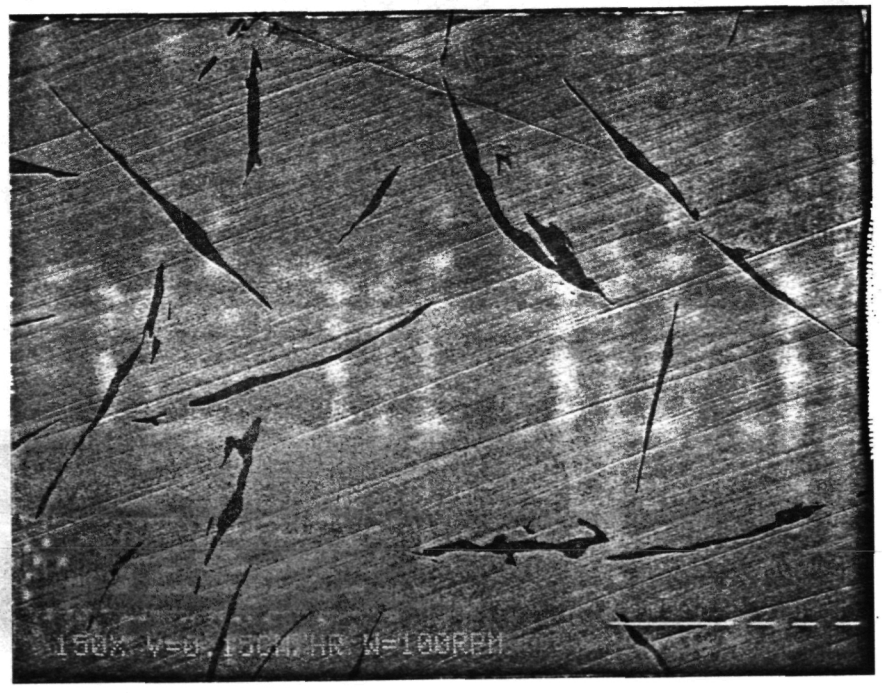

Figure 17. Scanning electron micrographs of transverse sections of MnBi/Bi eutectic solidified at 1.5 mm/hr, 150X.
Top - No rotation
Bottom - 100 RPM

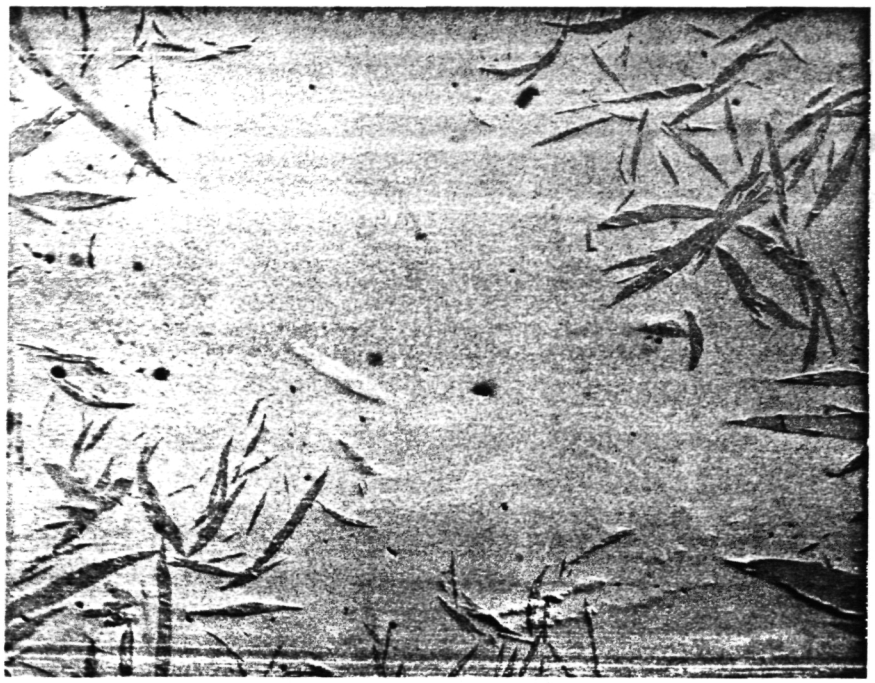

Figure 18. Cross-section of eutectic solidified at 1.5 mm/hr with 299 RPM rotation, 14X.

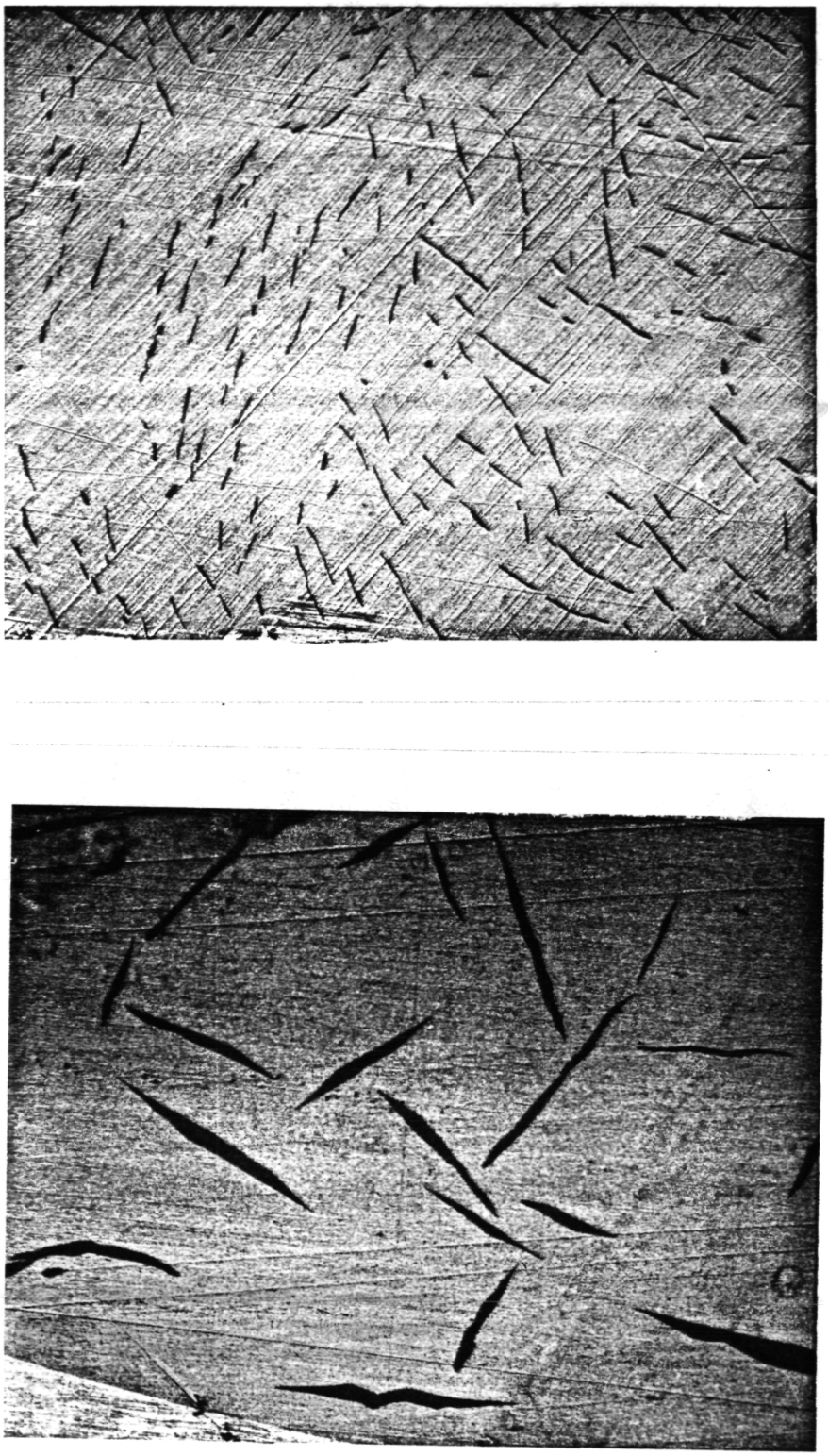

Figure 19. Eutectic solidified at 2.7 mm/hr, 150X.
Top - No rotation
Bottom - 100 RPM

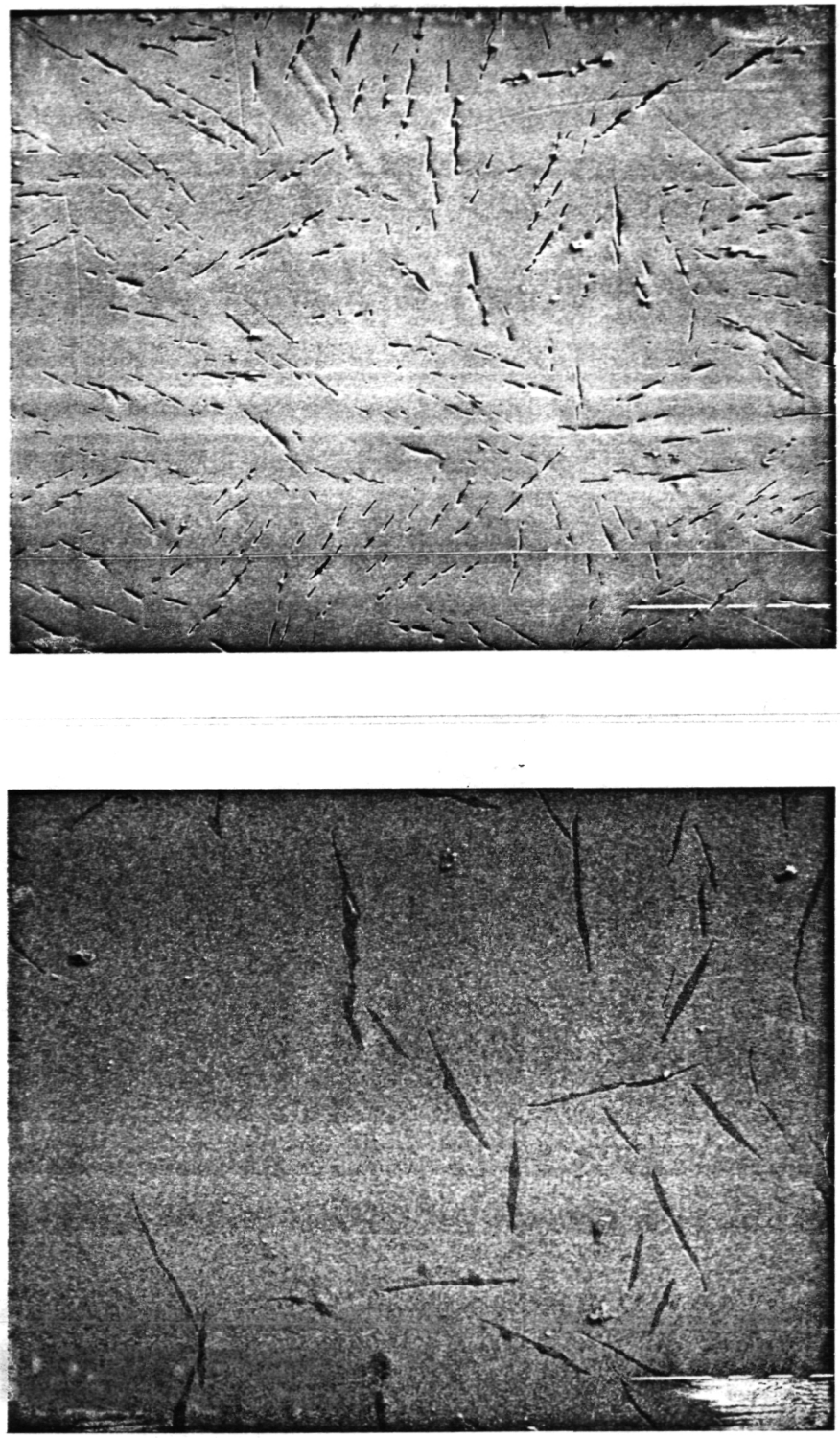

Figure 20. Eutectic solidified at 4.8 mm/hr, 200X.
Top - No rotation
Bottom 100 RPM

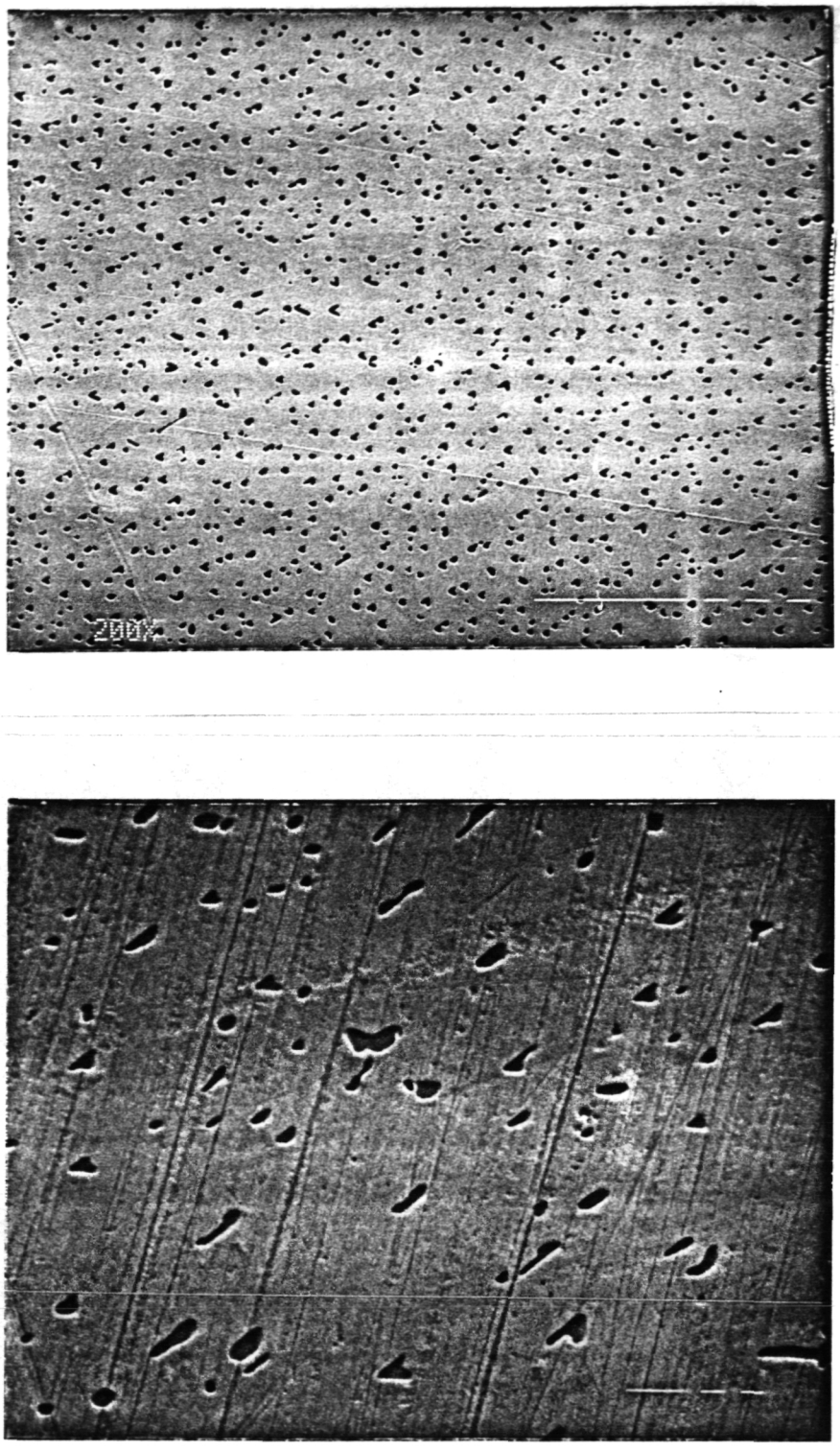

Figure 21. Eutectic solidified at 7.5 mm/hr, 200X.
Top - No rotation
Bottom - 100 RPM

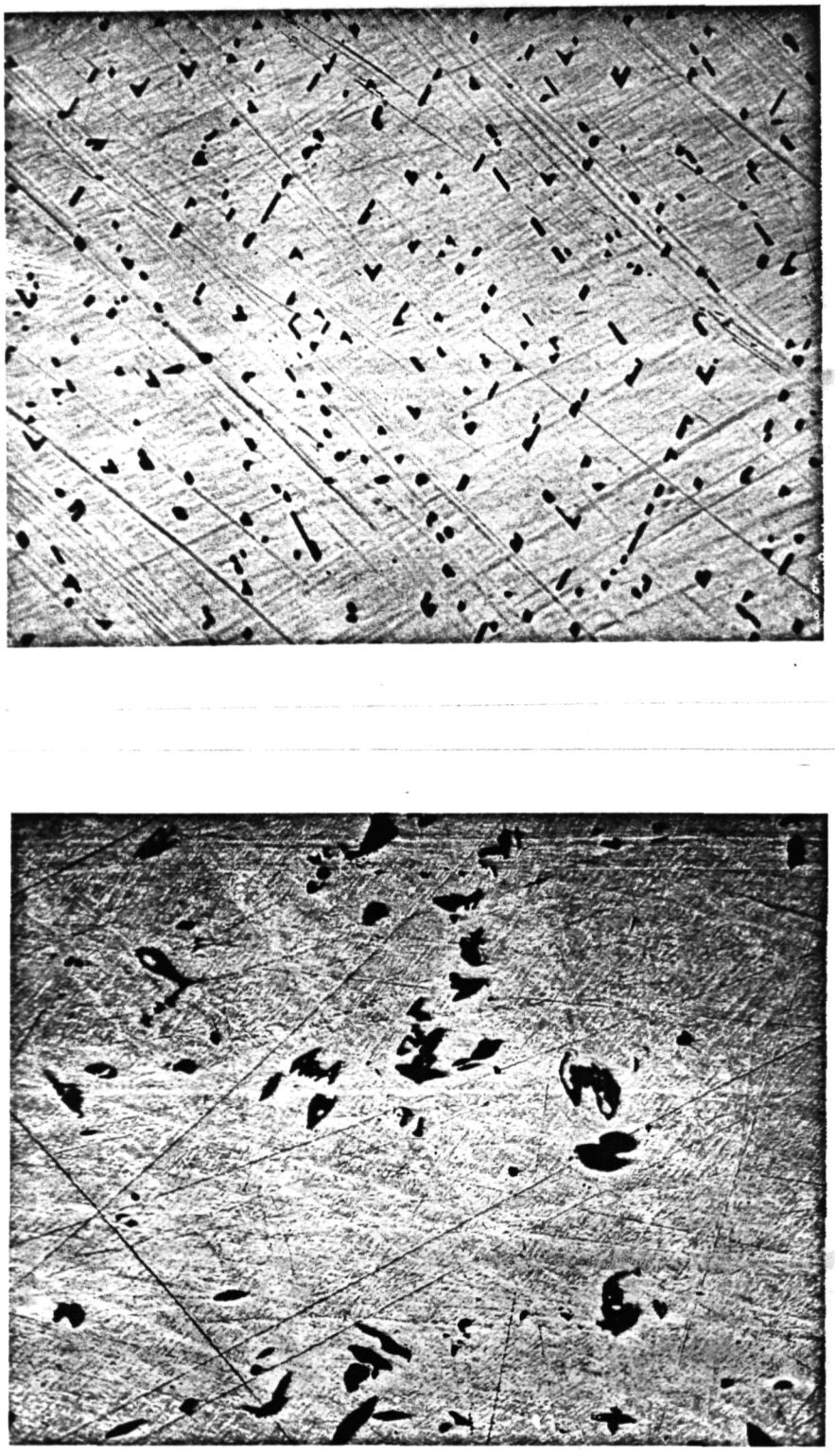

Figure 22. Eutectic solidified at 9 mm/hr, 500X.
Top - No rotation
Bottom - 100 RPM

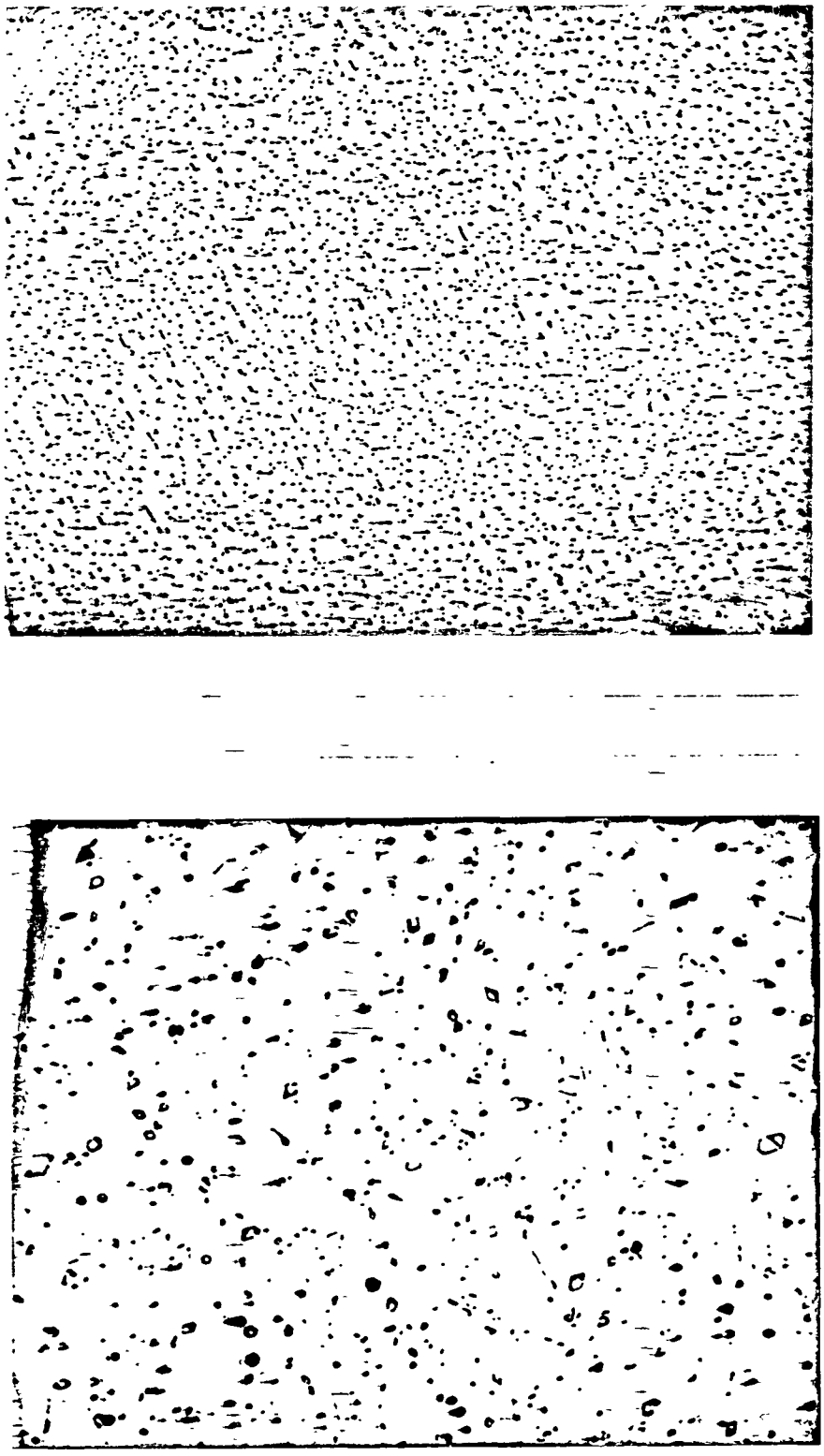

Figure 23. Eutectic solidified at 30 mm/hr, 300X.
Top - No rotation
Bottom - 100 RPM